Hindawi
Complexity
Volume 2020, Article ID 8231243, 10 pages
https://doi.org/10.1155/2020/8231243

Research Article

Online State of Charge Estimation of Lithium-Ion Cells Using Particle Filter-Based Hybrid Filtering Approach

Ming Zhang, Kai Wang, and Yan-ting Zhou

College of Electrical Engineering, Qingdao University, Qingdao 266071, China

Correspondence should be addressed to Kai Wang; wkwj888@163.com

Received 16 February 2019; Revised 13 May 2019; Accepted 15 June 2019; Published 10 January 2020

Academic Editor: Marcin Mrugalski

Filtering based state of charge (SOC) estimation with an equivalent circuit model is commonly extended to Lithium-ion (Li-ion) batteries for electric vehicle (EV) or similar energy storage applications. During the last several decades, different implementations of online parameter identification such as Kalman filters have been presented in literature. However, if the system is a moving EV during rapid acceleration or regenerative braking or when using heating or air conditioning, most of the existing works suffer from poor prediction of state and state estimation error covariance, leading to the problem of accuracy degeneracy of the algorithm. On this account, this paper presents a particle filter-based hybrid filtering method particularly for SOC estimation of Li-ion cells in EVs. A sampling importance resampling particle filter is used in combination with a standard Kalman filter and an unscented Kalman filter as a proposal distribution for the particle filter to be made much faster and more accurate. Test results show that the error on the state estimate is less than 0.8% despite additive current measurement noise with 0.05 A deviation.

1. Introduction

Li-ion battery based energy storage technology has become a key enabler of power grids grid and electric transportation sector objectives due to their beneficial properties [1]. Technical challenges that arise in ensuring safe, reliable, and durable operation of Li-ion batteries for both stationary and vehicular applications demanding large amounts of energy and power, have pushed the limit of battery technology and require development of sophisticated battery management system (BMS) [2–5].

Accurate SOC estimation plays an indispensable role in the design of control strategies and performance optimization for a BMS in a battery system. As a critical indicator of available energy in a Li-ion cell, SOC cannot be directly measured. Fortunately, it can be obtained by various estimation approaches based on coulomb counting, open circuit voltage (OCV), electrochemical impedance spectroscopy (EIS), or battery modelling approaches in combination with machine learning or modern control theory. During the last several decades, plenty of SOC estimation methods have been presented in literature [6–32]. In particular, latest comparative studies and reviews of most commonly used Li-ion cell SOC estimation approaches are presented in [33–40].

In [33], Lai et al. conduct a comparative analysis of eleven equivalent circuit models (ECMs) and SOC estimation errors and comparative study of the robustness of ECMs, in which the genetic algorithm was applied to carry out parameter identification and optimization and the EKF algorithm was used to estimate the SOC for a LiNMC battery in the new European driving cycle (NEDC). It is worth noting that the results show that the first-order and second-order RC models are the best choice for LiNMC batteries due to their balance of accuracy and reliability. Furthermore, Lai et al. undertake a comparative study for nine ECMs using nine optimizers in the entire SOC area by implementing model parameter optimization, and mention further works that need to be addressed for the design of sophisticated BMS in respect of accurate online identification of model parameters with less computational burden of a microcontroller [34]. In [35], Hannan et al. also conduct a comprehensive review of Li-ion battery SOC estimation and management system in EV applications in terms of challengers and recommendations.

So far, various approaches have been continuously being developed to increase the accuracy of SOC estimation and obtain a desirable stability and robustness at the same time. Equally important, the error sources of online SOC estimation methods need to be investigated. In [41], Zheng et al. use error

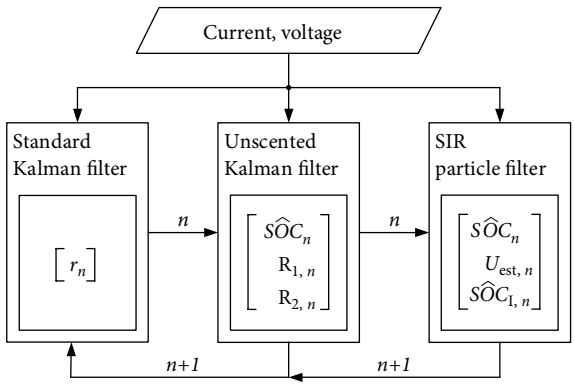

Figure 1: Framework of the proposed hybrid filtering algorithm.

flow charts to analyze SOC error sources from signal measurement to battery modelling and estimation algorithms.

Although Coulomb counting by itself offers better short-term accuracy, over the longer term it suffers from lack of an accurate reference point and unacceptable offset drift that severely degrades accuracy [7]. Therefore, Coulomb counting is usually used in combination with Kalman filter or Li-ion cell voltage translation for the EV applications.

EIS is a very powerful way to analyze the state of Li-ion cells and detect degradation of Li-ion cells by measuring impedance which requires an additional signal generator for various frequencies of sinusoidal alternating current or square waveform as input signals and additional computation for signal transformation from time domain to frequency domain [12, 13]. However, considering the time-intensive measurement and calculation as well as the remarkable impact of temperature and state of health (SOH) on the impedance change, the impedance spectroscopy method is not a practical choice for accurate SOC estimation in EV applications.

Alternatively, using an ECM of the battery, the SOC can be extracted by estimating the open circuit voltage (OCV) and then by using look-up tables which are usually available from the battery manufacturer. Also, artificial intelligence methods such as neural networks or fuzzy logic can be used for SOC estimation [17–19]. Model-based methods that use both the measured current and voltage can be used together with online parameter identification, such as Kalman filters, which is the most commonly used so far. The method introduced by Plett in [42–44] has resulted in various implementations of Kalman filter based SOC estimation for EVs. Particle filter based SOC estimation method is recently proposed for a better performance in [21–25].

In the field of battery modelling, although physics based electrochemical models can predict the spatially distributed behavior of the essential states of the battery, the required online computation becomes a time-consuming task for microcontroller-based BMS. Therefore, it is still a challenge to design and build accurate online SOC estimation algorithms for the BMS in terms of reduction of the full electrochemical model given by partial differential equations and algebraic equations, while getting desirable accuracy and computational speed. In [2], a detailed description and electrochemical model of a Li-ion battery is presented from a control perspective.

For simplification of electrochemical models, the Li-ion battery model is reformulated to facilitate computation. In [45], Han et al. introduce an improved single particle model (SPM) with high precision and the same level of computations as the original SPM and develop a simplified pseudo two-dimensional model. Bizeray et al. applied the EKF algorithm to the thermal-electrochemical P2D model solved using Chebyshev orthogonal collocation for battery state estimation in Bizeray et al. [46].

To reduce the voltage error and provide satisfactory estimation accuracy in the low SOC area, an extended ECM based on the SPM using the knowledge of the surface SOC is proposed in [47] and presents a better fitting result than the ECM at SOC lower than 20% by using the genetic algorithm for model parameter identification. However, errors in the SPM occur for either large values of applied current or during relaxation after applying a current pulse with a longer duration since the SPM does not model spatial variation of the states in the cell. These spatial variations become more prominent in the cell for either large currents or for long-duration pulses.

Based on the above literature review, to our knowledge, SOC estimation algorithms based on ECM and KF will still be preferred for a BMS in EV applications. In order to accurately estimate the effect of linear and nonlinear parameters on the SOC estimation separately and further achieve unbiased estimates based on the probability density evaluation of possible SOC true-value, a particle filter-based hybrid filtering approach is proposed in this paper. In the proposed algorithm, the Li-ion cell SOC is preliminary estimated by the coupled Kalman filter combining standard Kalman filter with unscented Kalman filter (UKF) to account for the linear and nonlinear effect of model parameters. In addition, the particle filtering algorithm is integrated into the proposed algorithm for correction of the SOC estimates based on the estimated probability density of possible SOC true-value. Finally, comprehensive tests including pulse charging test, Urban Dynamometer Driving Schedule (UDDS) test, and mixed charge and discharge test are conducted to validate the rationality and effectiveness of the proposed algorithm.

2. Implementation of the Proposed Hybrid Filtering Algorithm

In this section, the particle filter-based hybrid filtering approach is explained in detail. The schematic flowchart of the proposed algorithm is illustrated in Figure 1. Standard Kalman filter is responsible for estimating the main circuit resistor of the ECM. On this basis, the preliminary SOC and the polarization parameters are estimated simultaneously by the unscented Kalman filter. Finally, ampere-hour based, OCV based and model based SOC estimation methods are combined in the SIR particle filter, and the unbiased correction is derived. Apart from improving the SOC estimation accuracy, the idea of fusing different approaches offers a framework for the development of advanced and intelligent estimation algorithms.

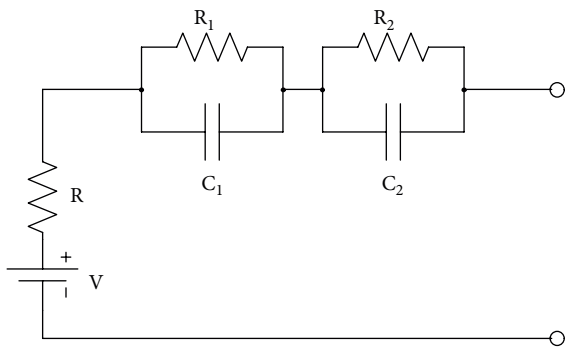

Figure 2: Equivalent circuit model of the Li-ion cell.

2.1. Li-Ion Cell Equivalent Circuit Model. In this work, a dual-polarization equivalent model of lithium-ion batteries is utilized to assist with the estimation of the equivalent resistor and polarization parameters which is essential for the preliminary SOC estimation based on UKF. The ECM of a Li-ion cell is shown in Figure 2. The battery voltage is formulated by Equation (1), the differential equations for the two RC circuits are expressed by Equations (2)–(3), and U_r can be expressed by Equation (4).

$$U = U_{OCV} + U_r + U_{C_1} + U_{C_2}, \tag{1}$$

$$U_{C_{1,k+1}} = U_{C_{1,k}} e^{-\Delta t/R_1C_1} + I_k R_1\left(1 - e^{-\Delta t/R_1C_1}\right), \tag{2}$$

$$U_{C_{2,k+1}} = U_{C_{2,k}} e^{-\Delta t/R_2C_2} + I_k R_2\left(1 - e^{-\Delta t/R_2C_2}\right), \tag{3}$$

$$U_r = I_k r_k, \tag{4}$$

wherein, U is the measured voltage, U_{OCV} is the open-circuit voltage, U_r is the voltage drop caused by the impedance on the main circuit, U_{c1} and U_{c2} are the voltage drops caused by the resistor-capacitor (RC) circuits, k is the measurement time-step.

Now, all items in (1) are given directly or by iteration except for U_{OCV}. U_{OCV} will be given by SOC–OCV curve in the following subsection.

2.2. SOC–OCV Curve. Open circuit voltage (OCV) is the steady voltage after the battery rests for a long time. The relationship between SOC and OCV is distinct for different Li-ion batteries, and the mapping between SOC and OCV for a specific kind of battery is unique. Moreover, such mapping remains unchanged during the battery service life, enabling a reliable SOC estimation. However, the definition of OCV prevents us from making use of OCV in online applications.

Here, pulse charging/discharging procedure is employed to obtain the expected SOC–OCV curve. The pulse charging/discharging result is obtained by using an industrial battery and cell test equipment in Figure 3.

The upper curve represents the data of pulse charging test, while the lower one results from the pulse discharging experiment. By fitting the data from the tests, the polarization effect

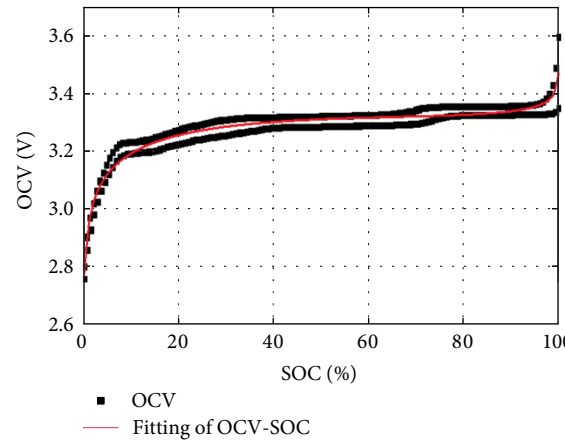

Figure 3: SOC–OCV curve of the Li-ion cell under test.

of battery is minimized and the SOC–OCV curve can be derived, recorded as OCV = f(SOC). Therefore, Equation (1) can be rewritten as Equation (5), which is the complete description of the Li-ion cell ECM as shown in Figure 2.

$$U_k = f(SOC) + I_k r_k + U_{C_{1,k}} + U_{C_{2,k}}. \tag{5}$$

However, it is worth noting that the difference between the upper and lower curve becomes more and more significant when SOC reaches about 0.95, resulting in inaccurate f(SOC).

2.3. Coupled Kalman Filter. After the measurement model as formulated in Equation (5) has been obtained, the coupled Kalman filter is designed by combing a standard Kalman filter and a UKF. The standard Kalman filter is supposed to estimate the value of the main circuit resistor r_k iterated, while the UKF is utilized to estimate the value of SOC and RC circuit parameters.

It should be mentioned that, as standard Kalman filter is based on linear Gaussian state-space model and it suffers from the divergence phenomenon, only the main circuit resistor r is estimated by it, while the polarization parameters, that is, RC parameter and SOC are estimated simultaneously by unscented Kalman filter.

2.3.1. Standard Kalman Filter. The standard KF can be constructed as follows:

System state

$$x_n = [\,U_{C_1,n} \quad U_{C_2,n} \quad r_n\,]^T. \tag{6}$$

Observation

$$y_n = Voltage_n - U_{OCV,n}. \tag{7}$$

Parameters in transition equation of system state is

$$A_n = \begin{bmatrix} e^{-dt/R_{1,n}C_{1,n}} & 0 & 0 \\ 0 & e^{-dt/R_{2,n}C_{2,n}} & 0 \\ 0 & 0 & 1 \end{bmatrix}, \quad B_n = \begin{bmatrix} R_{1,n}\left(1 - e^{-dt/R_{1,n}C_{1,n}}\right) \\ R_{2,n}\left(1 - e^{-dt/R_{2,n}C_{2,n}}\right) \\ 0 \end{bmatrix}. \tag{8}$$

$$\begin{cases} \tau_1 = R_{1,n}C_{1,n} = 0.02, \\ \tau_2 = R_{2,n}C_{2,n} = 1. \end{cases} \tag{9}$$

System control input:

$$u_{n-1} = I_{n-1}. \tag{10}$$

Measurement matrix:

$$H = [\,1 \quad 1 \quad I_n\,]. \tag{11}$$

Predicted measurement:

$$\widehat{z}_n = H_{n-1}\widehat{x}_{n|n-1}. \tag{12}$$

With Equations (6)–(12), the algorithm of standard Kalman filter can be implemented. In Equation (8), the time constants of the 2 RC circuits are fixed as Equation (9). The two constants consist of smaller and greater values in order to ensure that the short-term and long-term polarization effects can be simulated as closely as possible. On one hand, the current of the battery is supposed to be relatively small; then the smaller time constants may provide quick respond of polarization voltage. On the other hand, long-range polarization voltage can be maintained if the current is relatively high. Besides, $U_{C1,n}$ and $U_{C2,n}$ should not be changed by the KF to ensure that voltage differential equations (2) and (3) are satisfied. Therefore, system state update equation in the algorithm of the standard Kalman filter needs to be replaced by Equation (13).

$$\begin{cases} \widehat{x}_{n|n} = \widehat{x}_{n|n-1} + WK_nW^T\left(y_n - H_{n-1}\widehat{x}_{n|n-1}\right), \\ W = [\,0 \quad 0 \quad 1\,]. \end{cases} \tag{13}$$

2.3.2. Unscented Kalman Filter. In the previous section, the voltages of the capacitors are iterated and the main circuit impedance is estimated by standard Kalman Filter, which can merely deal with linear estimation. The dynamics of remaining parameters in the ECM, including resistors in RC circuits and SOC, may be more difficult and highly nonlinear, and the nonlinear estimation is required. By adopting deterministic sampling approach, UKF which can achieve higher order accuracy than EKF is preferable for the estimation of these parameters.

As the time-varying polarization effect is mainly characterized by the resistors in RC circuits, UKF can be applied to estimate R_1 and R_2. The standard KF can be constructed as follows:

System state:

$$x_n = [\,S\widehat{O}C_n \quad R_{1,n} \quad R_{2,n}\,]^T. \tag{14}$$

Observation:

$$y_n = \begin{bmatrix} Voltage_n - U_{C_1,n} - U_{C_2,n} - U_{r,n} \\ U_{C_1,n} \\ U_{C_2,n} \end{bmatrix}. \tag{15}$$

System control input:

$$u_{n-1} = I_{n-1}. \tag{16}$$

Parameters in transition equation of system state are in (17), where Capacity is the rated capacity of the battery. The capacity remains constant in the algorithm.

$$A = I, B = \begin{bmatrix} \dfrac{dt}{Capacity} & 0 & 0 \end{bmatrix}^T. \tag{17}$$

Measurement function:

$$\widehat{y}_{n|n-1} = \begin{bmatrix} f\left(S\widehat{O}C_n\right) \\ U_{C_1,n}e^{-\Delta t/\tau_1} + I_{n-1}R_{1,n}\left(1 - e^{-\Delta t/\tau_1}\right) \\ U_{C_2,n}e^{-\Delta t/\tau_2} + I_{n-1}R_{2,n}\left(1 - e^{-\Delta t/\tau_2}\right) \end{bmatrix}. \tag{18}$$

With Equations (14)–(18), the algorithm of UKF can be implemented.

2.4. Correction by SIR Particle Filter. For nonlinear state-space models, where both system model and measurement model are nonlinear, there are basically two approaches to compute an approximate solution, local approximation and global approximation. Rather than approximating around localized estimates of the system state, global approximation formulates the solution in a Bayesian estimation framework. SIP particle filter can be utilized to achieve global approximating, which is capable of estimating parameters of nonlinear models with nongaussian noise in real-time applications.

In the sampling procedure, a serial of particles and the corresponding weights are selected from the system state according to the importance distribution, after which the resampling can be conducted, using the corresponding weights to describe the discrete possibility distribution function.

The employment of SIR particle function introduces the following advantages.

(1) The SOC estimation results from coupled Kalman filters, and ampere-hour counter are regarded as possibility distributions. The former is used to draw samples, and the latter is reflected in selecting weights.

(2) Using the SOC estimated by coupled Kalman filters and the circuit model, the estimated battery voltage is descripted as a possibility distribution function. Together with the PDF from ampere-hour counter, the difference between the measured voltage and the PDF determines the weights of the samples.

(3) Model based, ampere-hour based and OCV based approaches are combined in the framework of SIR particle filters, which can handle highly nonlinear systems.

Detailed implementation of the correction by SIR particle filter is demonstrated below.

(1) Construct the importance distribution (19) using the $S\widehat{O}C_n$ and $P_{n|n}$ from previous section. Because the variance of SOC determines the dispersion of the particles, a greater variance will require larger number of particles to reach a steady estimation. For the consideration of computing effort, a coefficient k is introduced to narrow the covariant in Equation (20). The value of k, which we set it as 0.6, is a tradeoff of accuracy and computing speed.

$$\widehat{SOC}_n^{(i)} \sim N\left(\widehat{SOC}_n, P_{n|n}\right), \tag{19}$$

$$\widehat{SOC}_n^{(i)} \sim nN\left(\widehat{SOC}_n, kP_{n|n}\right), \qquad k = 0.6. \tag{20}$$

(2) With ampere-hour method, another SOC estimate is acquired for each particle of time $(n-1)$ in Equation (21). Hence a series of PDF is attained and the possibility of $\widehat{SOC}_n$ under each PDF is computed in Equation (22).

$$\widehat{SOC}_{I,n}^{(i)} = \widehat{SOC}_{n-1}^{(i)} + \frac{I_{n-1}dt}{Capacity}, \qquad i = 1, 2, \cdots, N, \tag{21}$$

$$p\left(\widehat{SOC}_n\right) = \frac{1}{\sqrt{2\pi P_{I,n|n}}} e^{-\left(\widehat{SOC}_n - \widehat{SOC}_{I,n}^{(i)}\right)^2 / 2P_{I,n|n}}, \qquad i = 1, 2, \cdots, N. \tag{22}$$

(3) According to SOC–OCV curve and the circuit model, the estimated voltage is shown in (23) for each particles, which can be further extended in to a PDF. The possibility of the real voltage $Voltage_n$ in different PDFs is expressed in (24).

$$U_{est,n}^{(i)} = f\left(\widehat{SOC}_n^{(i)}\right) + U_{C_1,n} + U_{C_2,n}, \qquad i = 1, 2, \cdots, N. \tag{23}$$

$$p(Voltage_n) = \frac{1}{\sqrt{2\pi P_{U_{est,n}}}} e^{-\left(Voltage_n - U_{est,n}^{(i)}\right)^2 / 2P_{U_{est,n}}}, \qquad i = 1, 2, \cdots, N. \tag{24}$$

(4) The weights are given in (25), which is the combination of steps 2 and 3.

$$\tilde{w}_n^{(i)} = w_{n-1}^{(i)} \sqrt{p\left(\widehat{SOC}_n\right) p(Voltage_n)}, \qquad i = 1, 2, \cdots, N. \tag{25}$$

(5) Conduct the resampling algorithm.

(6) The outputs of the filter are (26) and (27).

$$SOC_n = \sum_{i=1}^{N} \widehat{SOC}_n^{(i)} w_n^{(i)}. \tag{26}$$

$$P_n = \sum_{i=1}^{N} w_n^{(i)} \left(\widehat{SOC}_n^{(i)} - SOC_n\right)\left(\widehat{SOC}_n^{(i)} - SOC_n\right)^T. \tag{27}$$

3. Experiment and Discussion

3.1. Methodology. In the experiments, the SOC is defined as 0 when the discharging current is less than 0.1 A under a 2.5 V constant voltage discharging process, and is defined as 1 when the charging current is lower than 0.1 A with a constant voltage of 3.65 V.

At the beginning of each experiment, the *SOC* is 0 or 1, which ensures the actual *SOC* (SOC_a) can be obtained at anytime during the test by applying the Coulomb counting. The mixture of current sequence is attained by a high precision battery testing system. The Gaussian noise is imported into the estimation algorithm together with the voltage sequence. Then, the performance of the algorithm is evaluated by comparing SOC_a and the estimated *SOC* (SOC_{est}). A quantified approach to evaluate the accuracy of SOC estimation is RMSE (root-mean-square error) in Equation (28). Because the range of *SOC* is 0 to 1, thus the RMSE applied here has already been normalized.

$$RMSE = \sqrt{\frac{\sum_{t=1}^{n} \left(\hat{y}_t - y_t\right)^2}{n}}. \tag{28}$$

The initial estimated SOC in the algorithm is set as 0.6. It is worth noting that any initial between 0 and 1 is viable for the algorithm. The battery used is 18650 Li-ion cell with the rated capacity of 1300 mAh. The three types of experiments are as follows:

(1) 0.1 A pulse charging test for verifying the response performance of the algorithm, with relatively small current.

(2) UDDS test for simulating a driving test.

(3) Mixed charging/discharging test for evaluating the algorithm in extreme conditions.

3.2. Pulse Charging Test. At the beginning of pulse charging test, SOC_a equals to 0. The deviation of the white noise (σ_I^2) added in the current sequence is 0.0001 A. The testing procedure is as follows:

(1) Discharge with constant current 0.65 A until the cell voltage reaches 2.5 V.

(2) Discharge with constant voltage 2.5 V until the discharging current drops below 0.1 A.

(3) Rest for 10 hour

(4) Charge with 0.1 A for 5 mins.

(5) Rest for 10 mins.

(6) Repeat 4 and 5 until voltage reach 4.2 V.

(7) End.

At the end of step 3, the battery is fully discharged ($SOC_a = 0$), while at step 7, the battery is fully charged ($SOC_a = 1$). When the particle number N is 100, the overall result is shown in Figures 4 and 5.

With the same test data, the algorithm ran 100 times to validate the robustness of particle filter. The RMSE and the standard deviation are shown in Equation (29). Similarly, the RMSE mentioned in the rest of the paper is the result of 100 tests. The overall RMSE is lower than 1%, which is sufficient in most online applications. The oscillation appears at around SOC = 1 is probably because of the error of SOC–OCV curve mentioned in Section 2.2, which can be eliminated with precise SOC–OCV measurement. Another advantage of the algorithm proposed in the paper exhibits extremely quick response, shown in Figure 5. It takes merely 2 seconds for the algorithm to reach the steady value (around 0), starting from the initial value 0.6.

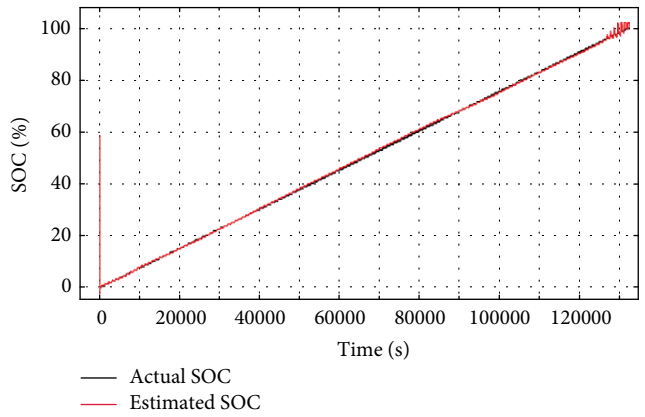

Figure 4: Estimated and actual SOCs under pulse charging test.

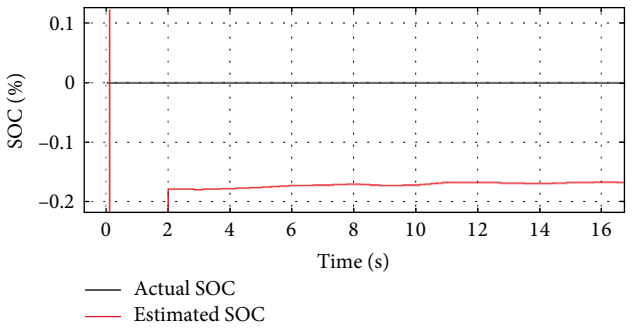

Figure 5: The SOC estimation within the very first 16 seconds under pulse charging test.

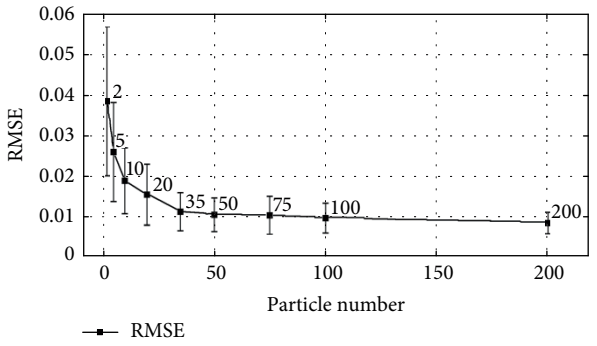

Figure 6: RMSE with different particle numbers under pulse charging test.

$$RMSE = 0.009567,$$
$$\sigma = 0.003671. \quad (29)$$

In particle filter, the number of particles determines the accuracy and speed of the algorithm. Figure 6 demonstrates the RMSE of the same pulse charging test, at different particle numbers. It is obvious that more particles result in higher accuracy. In an extreme case, Equation (30) is the result when particle number is set to 500, which represents the highest accuracy this algorithm can achieve. However, the computing effort increases dramatically as the number increases. To reach a balance at the tradeoff, number between 25 and 100 will be a good choice.

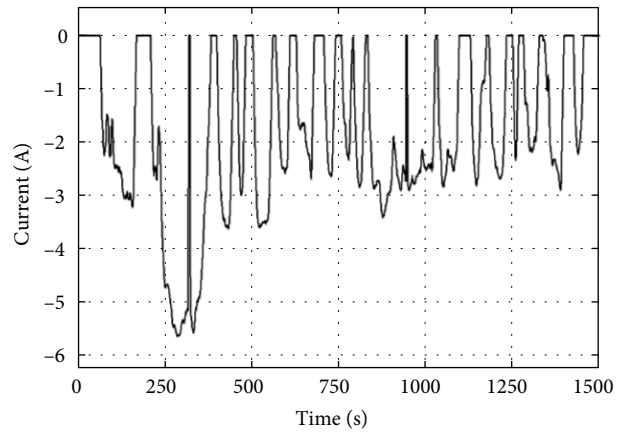

Figure 7: Cell current under UDDS test.

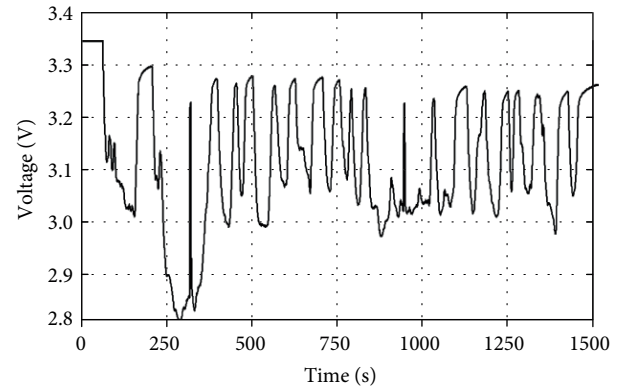

Figure 8: Cell voltage under UDDS test.

$$RMSE = 0.007364,$$
$$\sigma = 0.002124. \quad (30)$$

3.3. UDDS Test. As a dynamometer test, UDDS test represents city driving conditions, which is frequently used for light duty vehicle testing. The original UDDS descripts a speed-time chart, which is translated into the relation of current and time in this experiment. The current and voltage of the Li-ion cell under UDDS test is shown in Figures 7 and 8, respectively. In this simulation, current and voltage vary sharply, which should be a challenge to SOC estimation. Besides, the deviation white noise (σ_I^2) added into the current sequence is 0.05 A.

$$RMSE = 0.004773,$$
$$\sigma = 0.002712. \quad (31)$$

Figures 9 and 10 are the details of the test result and RMSE of 100 particles are shown in Equation (31). Similar to pulse charging test, the algorithm expresses the ability of quick responding. Meanwhile, it is interesting that the performance of algorithm is even better than that in pulse charging test. A possible explanation is that the algorithm is sensitive to the scale of current. The algorithm may rely more on voltage if the

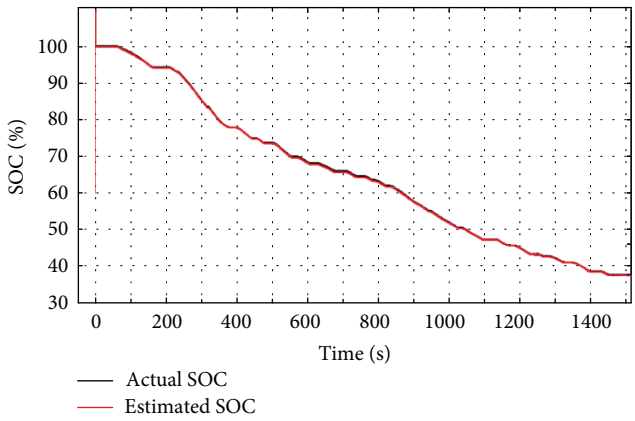

Figure 9: Estimated SOC and actual SOC under UDDS test.

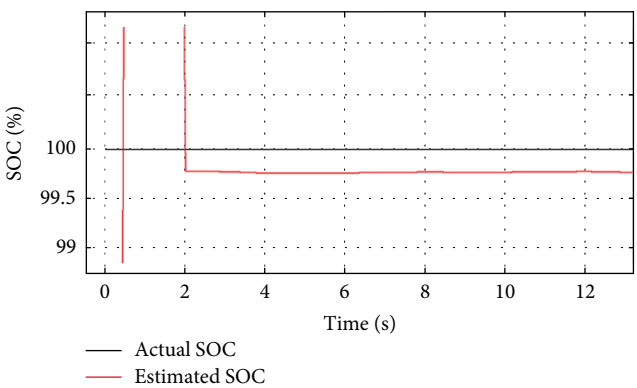

Figure 10: The SOC estimation within the very first 16 seconds under UDDS test.

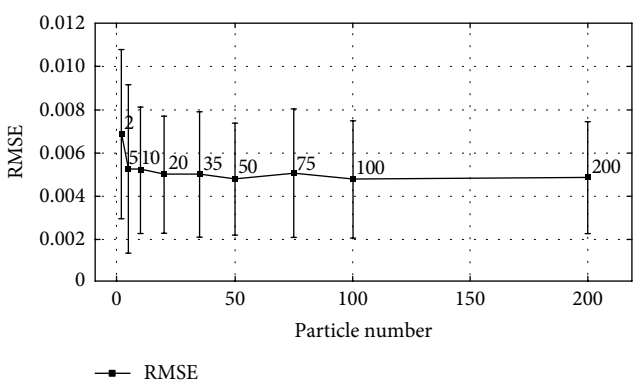

Figure 11: RMSE with different particle numbers under UDDS test.

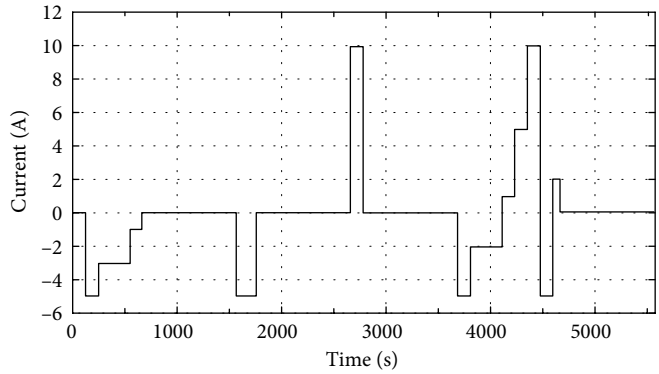

Figure 12: Cell current under mixed charging/discharging test.

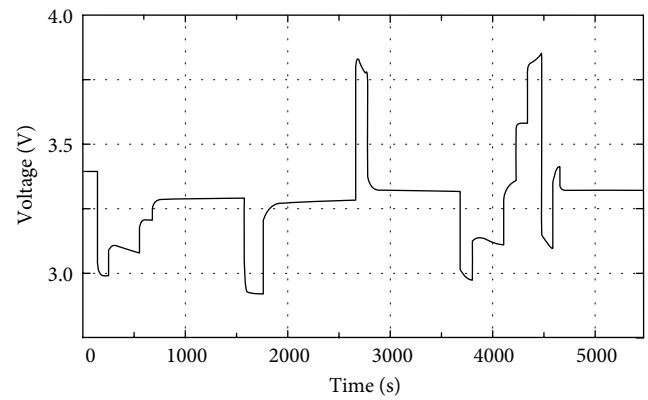

Figure 13: Cell voltage under mixed charging/discharging test.

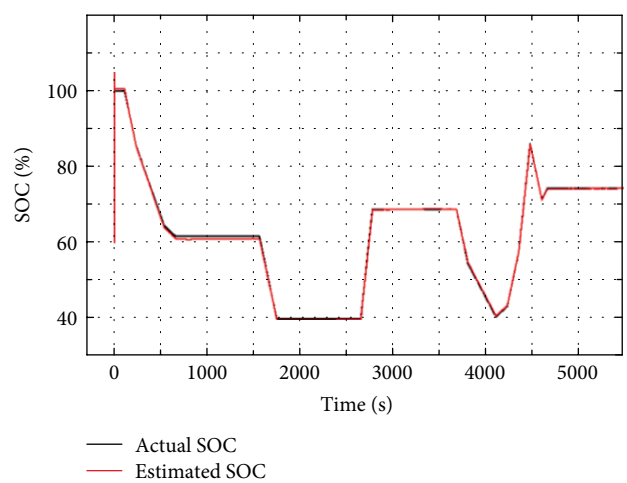

Figure 14: Estimated SOC and actual SOC under mixed charging/discharging test.

current is relatively small, which may possibly lead to larger error. In Figure 11, the trend of larger number leading to smaller error is less significant, comparing to that of pulse charging test.

3.4. Mixed Charging/Discharging Test. In the last two sections, the experiments are pure charging or discharging, while in this section, a mixed charging and discharging test is conducted, with current as high as 10 A, which is nearly the limitation of the battery. The deviation white noise (σ_I^2) added into the current sequence is 0.05 A. The current and voltage of the Li-ion cell under mixed charging/discharging test are shown in Figures 12 and 13, while the results are shown in Figures 14 and 15, and equation (32). The algorithm remains steady and accurate in such extreme conditions. In Figure 14, the

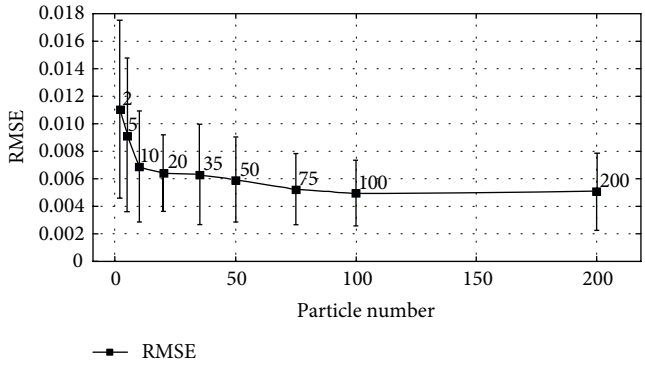

Figure 15: RMSE with different particle numbers under mixed charging/discharging test.

estimation error is relatively at the middle of the test, but it was eliminated later.

$$RMSE = 0.004891, \quad \sigma = 0.002422. \tag{32}$$

4. Conclusions

In this paper, a hybrid trilaminar filtering based SOC estimation algorithm is proposed with the combination of standard KF, UKF, and SIR particle filter. The coupled Kalman filtering algorithm is designed to obtain the preliminary SOC estimation value based on the typical ECM. On this basis, the estimated SOC is effectively corrected by the SIR Particle Filter to achieve the expected unbiased estimation based on the probability density evaluation of SOC true-value.

After various experiments, the algorithm is proved to be accurate enough for online applications. When the particle number is set to 100, the overall RMSE is lower than 1%, which can be improved to less than 0.8% if more particles are calculated. Also, the responding period is as short as 2 seconds. The only information needed in the algorithm is the SOC–OCV curve of a Li-ion cell. Based on the SOC estimation algorithm in this study, dynamic battery model is worth deeper investigation in order to reduce the dependence on SOC–OCV data.

Data Availability

The data used to support the findings of this study are available from the corresponding author upon request.

Conflicts of Interest

The authors declare that they have no conflicts of interest.

Acknowledgments

This work was performed under Shandong Provincial Key Research and Development Project. The authors would like to express their gratitude to the Department of Science and Technology of Shandong Province, the People's Republic of China, for the financial support under Grant No. 2019GGX103022. In addition, the authors have benefited a lot from closer collaborations with researcher and partners regarding their works [48–57] in the field of electrical engineering, electrochemical engineering, and materials science and engineering.

References

[1] P. W. Parfomak, "Energy storage for power grids and electric transportation: a technology assessment," *CRS Report for the US Congress*, 2012.

[2] N. A. Chaturvedi, R. Klein, J. Christensen, J. Ahmed, and A. Kojic, "Algorithms for advanced battery-management systems," *IEEE Control Systems Magazine*, vol. 30, pp. 49–68, 2010.

[3] M. T. Lawder, B. Suthar, P. W. C. Northrop et al., "Battery energy storage system (BESS) and battery management system (BMS) for grid-scale applications," *Proceedings of the IEEE*, vol. 102, pp. 1014–1030, 2014.

[4] F. Helling, S. Götz, and T. Weyh, "A battery modular multilevel management system (BM3) for electric vehicles and stationary energy storage systems," in *2014 16th European Conference on Power Electronics and Applications*, pp. 1–10, IEEE, Lappeenranta, Finland, 2014.

[5] C. Campestrini, M. F. Horsche, I. Zilberman, T. Heil, T. Zimmermann, and A. Jossen, "Validation and benchmark methods for battery management system functionalities: state of charge estimation algorithms," *Journal of Energy Storage*, vol. 7, pp. 38–51, 2016.

[6] Y. Xing, W. He, M. Pecht, and K. L. Tsui, "State of charge estimation of lithium-ion batteries using the open-circuit voltage at various ambient temperatures," *Applied Energy*, vol. 113, pp. 106–115, 2014.

[7] K. S. Ng, C. S. Moo, Y. P. Chen, and Y. C. Hsieh, "Enhanced coulomb counting method for estimating state-of-charge and state-of-health of lithium-ion batteries," *Applied Energy*, vol. 86, no. 9, pp. 1506–1511, 2009.

[8] Y. Tian, B. Z. Xia, W. Sun, Z. H. Xu, and W. W. Zheng, "A modified model based state of charge estimation of power lithium-ion batteries using unscented kalman filter," *Journal of Power Sources*, vol. 270, pp. 619–626, 2014.

[9] Q. Chen, J. C. Jiang, S. J. Liu, and C. P. Zhang, "A novel sliding mode observer for state of charge estimation of EV lithium batteries," *Journal of Power Electronics*, vol. 16, no. 3, pp. 1131–1140, 2016.

[10] X. Hu, S. Li, and Y. Yang, "Advanced machine learning approach for lithium-ion battery state estimation in electric vehicles," *IEEE Transactions on Transportation Electrification*, vol. 2, no. 2, pp. 140–149, 2016.

[11] G. O. Sahinoglu, M. Pajovic, Z. Sahinoglu, Y. Wang, P. V. Orlik, and T. Wada, "Battery state-of-charge estimation based on regular/recurrent gaussian process regression," *IEEE Transactions on Industrial Electronics*, vol. 65, no. 5, pp. 4311–4321, 2018.

[12] T. Yokoshima, D. Mukoyama, K. Nakazawa et al., "Application of electrochemical impedance spectroscopy to ferri/ferrocyanide redox couple and lithium ion battery systems using a square wave as signal input," *Electrochimica Acta*, vol. 180, pp. 922–928, 2015.

[13] K. Bundy, M. Karlsson, G. Lindbergh, and A. Lundqvist, "An electrochemical impedance spectroscopy method for prediction of the state of charge of a nickel-metal hydride battery at open circuit and during discharge," *Journal of Power Sources*, vol. 72, no. 2, pp. 118–125, 1998.

[14] S. Sepasi, R. Ghorbani, and B. Y. Liaw, "A novel on-board state-of-charge estimation method for aged Li-ion batteries based on model adaptive extended kalman filter," *Journal of Power Sources*, vol. 245, pp. 337–344, 2014.

[15] J. Xu, C. C. Mi, B. G. Cao, J. J. Deng, Z. Chen, and S. Q. Li, "The state of charge estimation of lithium-ion batteries based on a proportional-integral observer," *IEEE Transactions on Vehicular Technology*, vol. 63, no. 4, pp. 1614–1621, 2014.

[16] H. Aung, K. S. Low, and S. T. Goh, "State-of-charge estimation of lithium-ion battery using square root spherical unscented kalman filter (Sqrt-UKFST) in nanosatellite," *IEEE Transactions on Power Electronics*, vol. 30, no. 9, pp. 4774–4783, 2015.

[17] J. Chen, Q. Ouyang, C. Xu, and H. Su, "Neural network-based state of charge observer design for lithium-ion batteries," *IEEE Transactions on Control Systems Technology*, vol. 26, no. 1, pp. 313–320, 2018.

[18] D. Jiménez-Bermejo, J. Fraile-Ardanuy, S. Castaño-Solis, J. Merino, and R. Álvaro-Hermana, "Using dynamic neural networks for battery state of charge estimation in electric vehicles," *Procedia Computer Science*, vol. 130, pp. 533–540, 2018.

[19] E. Chemali, P. J. Kollmeyer, M. Preindl, and A. Emadi, "State-of-charge estimation of Li-ion batteries using deep neural networks: a machine learning approach," *Journal of Power Sources*, vol. 400, pp. 242–255, 2018.

[20] T. Zahid, K. Xu, W. Li, C. Li, and H. Li, "State of charge estimation for electric vehicle power battery using advanced machine learning algorithm under diversified drive cycles," *Energy*, vol. 162, pp. 871–882, 2018.

[21] A. Tulsyan, Y. Tsai, R. B. Gopaluni, and R. D. Braatz, "State-of-charge estimation in lithium-ion batteries: a particle filter approach," *Journal of Power Sources*, vol. 331, pp. 208–223, 2016.

[22] S. Schwunk, N. Armbruster, S. Straub, J. Kehl, and M. Vetter, "Particle filter for state of charge and state of health estimation for lithium–iron phosphate batteries," *Journal of Power Sources*, vol. 239, pp. 705–710, 2013.

[23] D. E. Acuña and M. E. Orchard, "Particle-filtering-based failure prognosis via sigma-points: application to lithium-ion battery state-of-charge monitoring," *Mechanical Systems and Signal Processing*, vol. 85, pp. 827–848, 2017.

[24] Z. Chen, H. Su, G. Dong, and J. Wu, "Particle filterbased state-of-charge estimation and remaining-dischargeable-time prediction method for lithium-ion batteries," *Journal of Power Sources*, vol. 414, pp. 158–166, 2019.

[25] D. M. Zhou, K. Zhang, A. Ravey, F. Gao, and A. Miraoui, "Online estimation of lithium polymer batteries state-of-charge using particle filter-based data fusion with multimodels approach," *IEEE Transactions on Industry Applications*, vol. 52, no. 3, pp. 2582–2595, 2016.

[26] D. J. Lim, J. H. Ahn, D. H. Kim, and B. K. Lee, "A mixed SOC estimation algorithm with high accuracy in various driving patterns of EVs," *Journal of Power Electronics*, vol. 16, no. 1, pp. 27–37, 2016.

[27] C. Zou, X. Hu, S. Dey, L. Zhang, and X. Tang, "Nonlinear fractional-order estimator with guaranteed robustness and stability for lithium-ion batteries," *IEEE Transactions on Industrial Electronics*, vol. 65, no. 7, pp. 5951–5961, 2018.

[28] B. Xia, C. Chen, Y. Tian, W. Sun, Z. Xu, and W. Zheng, "A novel method for state of charge estimation of lithium-ion batteries using a nonlinear observer," *Journal of Power Sources*, vol. 270, pp. 359–366, 2014.

[29] Y. Tian, C. R. Chen, B. Z. Xia, W. Sun, Z. H. Xu, and W. W. Zheng, "An adaptive gain nonlinear observer for state of charge estimation of lithium-ion batteries in electric vehicles," *Energies*, vol. 7, no. 9, pp. 5995–6012, 2014.

[30] Q. Yu, R. Xiong, C. Lin, W. Shen, and J. Deng, "Lithium-ion battery parameters and state-of-charge joint estimation based on H-infinity and unscented kalman filters," *IEEE Transactions on Vehicular Technology*, vol. 66, no. 10, pp. 8693–8701, 2017.

[31] J. Xie, J. Ma, Y. Sun, and Z. Li, "Estimating the state-of-charge of lithium-ion batteries using an H-infinity observer with consideration of the hysteresis characteristic," *Journal of Power Electronics*, vol. 16, no. 2, pp. 643–653, 2016.

[32] S. Li, C. Zou, M. Küpper, and S. Pischinger, "Model-based state of charge estimation algorithms under various current patterns," *Energy Procedia*, vol. 158, pp. 2806–2811, 2019.

[33] X. Lai, Y. Zheng, and T. Sun, "A comparative study of different equivalent circuit models for estimating state-of-charge of lithium-ion batteries," *Electrochimica Acta*, vol. 259, pp. 566–577, 2018.

[34] X. Lai, W. Gao, Y. Zheng et al., "A comparative study of global optimization methods for parameter identification of different equivalent circuit models for Li-ion batteries," *Electrochimica Acta*, vol. 295, pp. 1057–1066, 2019.

[35] M. A. Hannan, M. S. H. Lipu, A. Hussain, and A. Mohamed, "A review of lithium-ion battery state of charge estimation and management system in electric vehicle applications: challenges and recommendations," *Renewable and Sustainable Energy Reviews*, vol. 78, pp. 834–854, 2017.

[36] F. Yang, Y. Xing, D. Wang, and K. L. Tsui, "A comparative study of three model-based algorithms for estimating state-of-charge of lithium-ion batteries under a new combined dynamic loading profile," *Applied Energy*, vol. 164, pp. 387–399, 2016.

[37] J. Li, J. K. Barillas, C. Guenther, and M. A. Danzer, "A comparative study of state of charge estimation algorithms for $LiFePO_4$ batteries used in electric vehicles," *Journal of Power Sources*, vol. 230, pp. 244–250, 2013.

[38] J. K. Barillas, J. Li, C. Günther, and M. A. Danzer, "A comparative study and validation of state estimation algorithms for Li-ion batteries in battery management systems," *Applied Energy*, vol. 155, pp. 455–462, 2015.

[39] C. Campestrini, T. Heil, S. Kosch, and A. Jossen, "A comparative study and review of different kalman filters by applying an enhanced validation method," *Journal of Energy Storage*, vol. 8, pp. 142–159, 2016.

[40] H. S. Ramadan, M. Becherif, and F. Claude, "Extended kalman filter for accurate state of charge estimation of lithium-based batteries: a comparative analysis," *International Journal of Hydrogen Energy*, vol. 42, no. 48, pp. 29033–29046, 2017.

[41] Y. Zheng, M. Ouyang, X. Han, L. Lu, and J. Li, "Investigating the error sources of the online state of charge estimation methods for lithium-ion batteries in electric vehicles," *Journal of Power Sources*, vol. 377, pp. 161–188, 2018.

[42] G. L. Plett, "Extended kalman filtering for battery management systems of LiPB-based HEV battery packs: part 1. Background," *Journal of Power Sources*, vol. 134, no. 2, pp. 252–261, 2004.

[43] G. L. Plett, "Extended kalman filtering for battery management systems of LiPB-based HEV battery packs: part 2. Modeling

and identification," *Journal of Power Sources*, vol. 134, no. 2, pp. 262–276, 2004.

[44] G. L. Plett, "Extended kalman filtering for battery management systems of LiPB-based HEV battery packs: part 3. State and parameter estimation," *Journal of Power Sources*, vol. 134, no. 2, pp. 277–292, 2004.

[45] X. Han, M. Ouyang, L. Lu, and J. Li, "Simplification of physics-based electrochemical model for lithium ion battery on electric vehicle. Part II: pseudo-two-dimensional model simplification and state of charge estimation," *Journal of Power Sources*, vol. 278, pp. 814–825, 2015.

[46] A. M. Bizeray, S. Zhao, S. R. Duncan, and D. A. Howey, "Lithium-ion battery thermal-electrochemical model-based state estimation using orthogonal collocation and a modified extended kalman filter," *Journal of Power Sources*, vol. 296, pp. 400–412, 2015.

[47] M. Ouyang, G. Liu, L. Lu, J. Li, and X. Han, "Enhancing the estimation accuracy in low state-of-charge area: a novel onboard battery model through surface state of charge determination," vol. 270, pp. 221–237, 2014.

[48] K. Wang, J. B. Pang, L. W. Li, S. Z. Zhou, Y. H. Li, and T. Z. Zhang, "Synthesis of hydrophobic carbon nanotubes/reduced graphene oxide composite films by flash light irradiation," *Frontiers of Chemical Science and Engineering*, vol. 12, no. 3, pp. 376–382, 2018.

[49] K. Wang, L. W. Li, Y. Lan, P. Dong, and G. T. Xia, "Application research of chaotic carrier frequency modulation technology in two-stage matrix converter," *Mathematical Problems in Engineering*, vol. 2019, Article ID 2614327, 8 pages, 2019.

[50] K. Wang, S. Z. Zhou, Y. T. Zhou, J. Ren, L. W. Li, and Y. Lan, "Synthesis of porous carbon by activation method and its electrochemical performance," *International Journal of Electrochemical Science*, vol. 13, pp. 10766–10773, 2018.

[51] Y. T. Zhou, Y. N. Wang, K. Wang et al., "Hybrid genetic algorithm method for efficient and robust evaluation of remaining useful life of supercapacitors," *Applied Energy*, vol. 260, Article ID 114169, 2020.

[52] Y. T. Zhou, Y. N. Huang, J. B. Pang, and K. Wang, "Remaining useful life prediction for supercapacitor based on long short-term memory neural network," *Journal of Power Sources*, vol. 440, Article ID 227149, 2019.

[53] D. L. Yuan, C. Zhang, S. F. Tang et al., "Enhancing CaO_2 fenton-like process by Fe(II)-oxalic acid complexation for organic wastewater treatment," *Water Research*, vol. 163, Article ID 114861, 2019.

[54] K. Wang, L. W. Li, W. Xue et al., "Electrodeposition synthesis of PANI/MnO_2/graphene composite materials and its electrochemical performance," *International Journal of Electrochemical Science*, vol. 12, pp. 8306–8314, 2017.

[55] G. T. Xia, C. Li, K. Wang, and L. W. Li, "Structural design and electrochemical performance of PANI/CNTs and MnO_2/CNTs supercapacitor," *Science of Advanced Materials*, vol. 11, no. 8, pp. 1079–1086, 2019.

[56] K. Wang, L. W. Li, T. Z. Zhang, and Z. F. Liu, "Nitrogen-doped graphene for supercapacitor with long-term electrochemical stability," *Energy*, vol. 70, pp. 612–617, 2014.

[57] L. Zhao, L. Kang, and S. Yao, "Research and application of acoustic emission signal processing technology," *IEEE Access*, vol. 7, pp. 984–993, 2019.